Design of Interleaved BuckBoost DC-DC Converter using Loop Shaping Technique and Investigation of Converter through Time and Frequency Response

Vinayak Tripathi, Vaishali Chapparya, G. Murali Krishna,
Prakash Dwivedi, *Member, IEEE*, and Sourav Bose, *Member, IEEE*

***Abstract*—The response of DC-DC converters plays a vital role in performance of renewable energy exploitation systems. Therefore, this study presents a graphical loop shaping technique of non-minimal phase(NMP) unstable Interleaved Buck–Boost Converter(IBBC) for various micro grid SPV systems to help the designers for achieving the required performance with less ripples. A comparative analysis of transient and steady state response are also presented. To validate the performance of time response, frequency response analysis is presented. Finally the simulation results in MATLAB are used to reconfirm the validity of the presented analysis.**

***Index Terms*—Interleaved Buck-Boost Converter, Loop-shaping, Sensitivity, Non-minimal phase(NMP)**

I. Introduction

Nowadays when fossils fuel is degrading continuously, renewable energy is playing an important role in facing the continuous demand for electricity without damaging the environment. Generally, solar panels are widely used for producing electrical energy as it does not create any harm to the environment. The output of these panels is variable, therefore to achieve a constant output, Buck-Boost converters are used. DC-DC converters are important topology which can improve the performance of renewable energy sources [1]. DC-DC converters are used to change voltage levels of DC source from one level to other. These converters can both step-up or step-down the initial voltage [2]. In higher power rating inductor of Buck-Boost converter become bulkier. This inductor causes an increment in voltage and current ripple of the converter. In addition, most of the DC-DC converters have drawback of pulsating input and output current which creates high noise and makes control of system complicated due to current limitations [3]. To avoid these ripple and drawbacks without compromising power rating of the system an Interleaved Buck-Boost Converter can be used. In Interleaved Buck-Boost Converter inductors are placed in the parallel configuration so net inductance gets reduced. As inductance value has been reduced so voltage and current ripple will get reduced.

In present time Interleaved Buck-Boost Converters have been used in many applications like photo-voltaic energy applications (fuel cell, solar panels), electric vehicles etc.[4], [5], [6], [7], [8], [9], [10], [11], [12] because of its further advantages like harmonic cancellation, better efficiency, component stresses reduction, better thermal performance and high power density [3].

In the recent years various controllers using particle swarm optimization [13], BATA optimization tuned fuzzy sliding mode controller [14], GA-based robust LQR controller [15], FPGA-based optimal robust minimal-order controller structure [16] etc. have been used to control dc-to-dc Converter system. Although these controllers are good, but they required a complex mathematics. Here, an attempt has been made to design a compensator for a non-minimal phase open-loop unstable Interleaved Buck-Boost DC-DC Converter using a classical loop-shaping technique. It is noteworthy here, no loop-shaping technique has been reported in literature so far to design a controller for non-minimal phase system as well as for Buck-Boost Converters.

The content structure of the paper is as follows: SectionII provides mathematical modeling of Interleaved Buck-Boost Converter and controller design has been provided in SectionIII. Section IV includes the discussion and analysis of simulation results for controllers and Section V presents the concluding remarks.

II. Mathematical Modeling

A. Experimental Framework

The equivalent-circuit of Interleaved Buck–Boost Converter is shown in Fig.1.

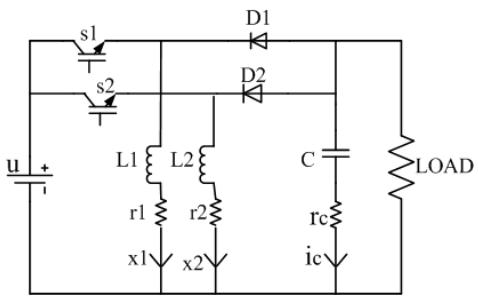

Fig. 1: circuit diagram of Interleaved Buck-Boost Converter

Vinayak Tripathi, Department of Electrical Engineering, National Institute of Technology, Uttarakhand, India. e-mail:tripathivinayak056@gmail.com
Vaishali Chapparya, Department of Electrical Engineering, National Institute of Technology, Uttarakhand, India. e-mail:kutku2093@gmail.com
G. Murali Krishna, Department of Electrical Engineering, National Institute of Technology, Uttarakhand, India. e-mail:muralikrishnagowra@gmail.com
Prakash Dwivedi, Department of Electrical Engineering, National Institute of Technology, Uttarakhand, India. e-mail:prakashdwivedi@nituk.ac.in
Sourav Bose, Department of Electrical Engineering, National Institute of Technology, Uttarakhand, India. e-mail:souravbose@nituk.ac.in

ISBN: 978-988-14048-8-6
ISSN: 2078-0958 (Print); ISSN: 2078-0966 (Online)

In the Fig.1 switches and diodes are practical devices with r_{s1}, r_{s2} and r_{d1}, r_{d2} resistances respectively. Inductors and capacitors are also practical devices with r_1 resistance in L_1, r_2 resistance in L_2 and r_c resistance in capacitor. In Buck-Boost Converter Buck and Boost mode can be defined according to value of duty-cycle(D). Here we are going to present modelling for Boost mode, similarly can be understood for Buck mode. According to switch-operations, four modes can be obtained which has been shown in Table I.

TABLE I: Different Modes of operation of IBBC

S_1	S_2	Mode
ON	ON	Mode - 1
ON	OFF	Mode - 2
OFF	ON	Mode - 3
OFF	OFF	Mode - 4

B. Governing Equations

The Mathematical-modeling of the IBBC in all four modes is carried out for getting average state-space model.

Mode-1: When both switches are ON, diode becomes

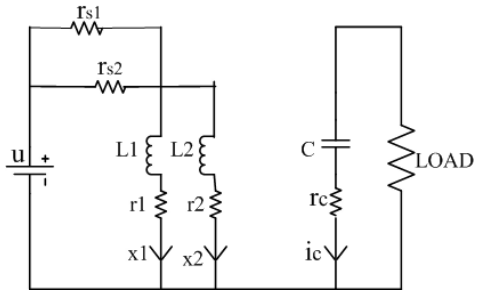

Fig. 2: circuit diagram of Interleaved Buck-Boost Converter when both switches are ON

reverse biased. In Mathematical equations, switch resistances are also considered. Resultant circuit diagram of $Mode1$ has shown in Fig. 2. Let u be the input of the Converter. x_1 is the current in L_1 and x_2 is current in L_2. Similarly current in capacitor denoted as i_c and voltage across it taken as x_3. Here x_1, x_2 and x_3 are state variables.

Apply KVL in first loop and get (1) and 2

$$u = L_1.\frac{dx_1}{dt} + r_1.x_1 + r_{s1}.x_1 \tag{1}$$

$$\frac{dx_1}{dt} = \frac{-(r_1 + r_{s1}).x_1}{L_1} + \frac{u}{r_1} \tag{2}$$

Apply KVL in second loop and get (3) and (4)

$$u = L_2.\frac{dx_2}{dt} + r_2.x_2 \tag{3}$$

$$\frac{dx_2}{dt} = \frac{-r_2.x_2}{L_2} + \frac{u}{r_2} \tag{4}$$

Apply KVL in third loop and get (5)

$$x_3 = i_o.R - i_c.r_c. \tag{5}$$

Here i_o is output current and R is load resistance.

Apply KVL in third loop and get (6)

$$i_o = -i_c \tag{6}$$

Equation (5) and (6) gives the (7)

$$\frac{dx_3}{dt} = \frac{-x_3}{C.(R + r_c)} \tag{7}$$

Using above equations we can define State-space model of $Mode1$ by comparing it with (8) and (9)

$$\frac{dx}{dt} = A.x + B.u \tag{8}$$

$$y = C.x + D.u. \tag{9}$$

Here A= State-space matrix
B= Input matrix
C= Output matrix
D= Feed-through (or feed-forward) matrix.
x= state vector
y= output vector
u= input(or control) vector
So,

Equation (10), (11), and (12), represents a state matrix, Input matrix, and Output Matrix respectively.

$$A_1 = \begin{bmatrix} \frac{-(r_1+r_{s1})}{L_1} & 0 & 0 \\ 0 & \frac{-(r_2+r_{s2})}{L_2} & 0 \\ 0 & 0 & \frac{-(1)}{C.(R+r_c)} \end{bmatrix} \tag{10}$$

$$B_1 = \begin{bmatrix} \frac{1}{L_1} & \frac{1}{L_1} & 0 \end{bmatrix}^T \tag{11}$$

$$C_1 = \begin{bmatrix} 0 & 0 & \frac{R}{R+r_c} \end{bmatrix} \tag{12}$$

Similarly the State-space models of other modes of operation are obtained and given in Eq. (13) to (21).

Mode-2:

$$A_2 = \begin{bmatrix} \frac{-(r_1+r_{s1})}{L_1} & 0 & 0 \\ 0 & \frac{-(r_{d2}+r_2+\frac{R.r_c}{R+r_c})}{L_2} & \frac{R}{L_2.(r_c+R)} \\ 0 & \frac{-R}{C.(R+r_c)} & \frac{-1}{C.(R+r_c)} \end{bmatrix} \tag{13}$$

$$B_2 = \begin{bmatrix} \frac{1}{l_1} & 0 & 0 \end{bmatrix}^T \tag{14}$$

$$C_2 = \begin{bmatrix} 0 & \frac{-r_c.R}{R+r_c} & \frac{R}{R+r_c} \end{bmatrix} \tag{15}$$

Mode-3:

$$A_3 = \begin{bmatrix} \frac{-(r_{d1}+r_1+\frac{R.r_c}{R+r_c})}{L_1} & 0 & \frac{R}{L_1(R+r_c)} \\ 0 & \frac{-(r_2+r_{s2})}{L_2} & 0 \\ \frac{-R}{C.(R+r_c)} & 0 & \frac{-1}{C.(R+r_c)} \end{bmatrix} \tag{16}$$

$$B_3 = \begin{bmatrix} 0 & \frac{1}{L_2} & 0 \end{bmatrix}^T \tag{17}$$

$$C_3 = \begin{bmatrix} \frac{-r_c.R}{R+r_c} & 0 & \frac{R}{R+r_c} \end{bmatrix} \tag{18}$$

ISBN: 978-988-14048-8-6
ISSN: 2078-0958 (Print); ISSN: 2078-0966 (Online)

Mode-4:

$$A_4 = \begin{bmatrix} \frac{-(r_1+\frac{R}{R+r_c})}{L_1} & \frac{-R}{L_1.(R+r_c)} & \frac{R}{L_1.(R+r_c)} \\ \frac{-R}{L_2.(R+r_c)} & \frac{-(r_2+\frac{R}{R+r_c})}{L_2} & \frac{R}{L_2.(R+r_c)} \\ \frac{-R}{C.(R+r_c)} & \frac{-R}{C.(R+r_c)} & \frac{-1}{C.(R+r_c)} \end{bmatrix} \quad (19)$$

$$B_4 = \begin{bmatrix} 0 & 0 & 0 \end{bmatrix}^T \quad (20)$$

$$C_4 = \begin{bmatrix} \frac{-R}{R+r_c} & \frac{-R}{R+r_c} & \frac{-(1+R+r_c)}{R+r_c} \end{bmatrix} \quad (21)$$

TABLE II: Design Requirement of Interleaved Buck-Boost Converter

Parameters Description	Notations	Experimental Value	Units
Source voltage	V_s	25	V
Output voltage	V_o	-50	V
Source current	I_s	2	A
Current through inductor L1	i_{l1}	3	A
Current through inductor L2	i_{l2}	3	A
Output current	I_o	1	A
Duty ratio	D/d	0.663	-
Switching frequency	f_s	50	KHz
Inductor L1 ripple current	$\triangle I_{l1}$	0.03	A
Inductor L2 ripple current	$\triangle I_{l2}$	0.03	A
Voltage ripple	$\triangle V_o$	0.5	V
Inductor	L1	44.1	mH
Inductor	L2	.1	mH
Capacitor	C	12.96	μF
Load Resistance	R	50	Ω

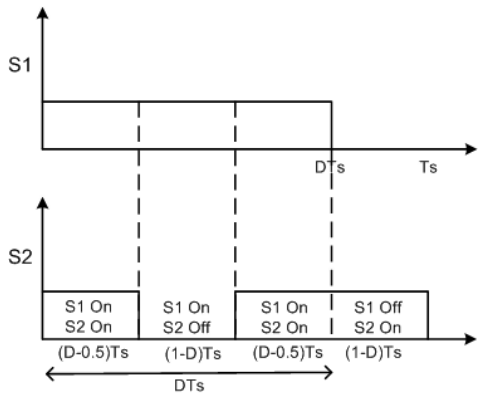

Fig. 3: Switching pattern of Interleaved Buck-Boost Converter for $D > 0.5$ (Boost Operation).

1) State apace averaging: By observing the switching pattern shown in Fig. 3, it is clear that $Mode1$ will operate for $(D-0.5).T_s$ time period, $Mode2$ will operate for $(1-D).T_s$ time period, $Mode3$ will operate for $(D-0.5).T_s$ time period and for this operating condition $Mode4$ will never happen. So Average State-space model over one particular cycle can be written as (22) and (23)

$$\frac{dx}{dt} = A.x + B.u \quad (22)$$

$$y = C.x + D.u \quad (23)$$

Where Equation (24), (25), and (26), represents a state matrix, Input matrix, and Output Matrix.

$$A = \sum_{j=1}^{N} d_j.A_j \quad (24)$$

$$B = \sum_{j=1}^{N} d_j.B_j \quad (25)$$

$$C = \sum_{j=1}^{N} d_j.C_j \quad (26)$$

Here, d is defined as duty cycle.

If d is constant, it is defined as Steady-State duty ratio D. From Fig. 3 and equations (22)-(26), the state-space matrices are opted and can be written as in (27), (28), and (29).

$$A = A_1.(2D-1) + (A_2+A_3).(1-D) \quad (27)$$

$$B = B_1.(2D-1) + (B_2+B_3).(1-D) \quad (28)$$

$$C = C_1.(2D-1) + (C_2+C_3).(1-D) \quad (29)$$

C. Small-signal Analysis

To analyze small-signal behavior, it is assumed that d varies from cycle to cycle. Equation (30) can be opted by introducing noise and disturbances in (22).

$$\dot{X} = A.X + B.U \quad (30)$$

Here,

$$\dot{X} = \dot{x} + \hat{\dot{x}} \quad (31)$$

$$U = u + \hat{u} \quad (32)$$

$$d = D + \hat{d} \quad (33)$$

put (31)-(33) in (30) will give the (34), Here,

$$\begin{aligned} \dot{x} + \hat{\dot{x}} = [(A_1.(2(D+\hat{d})-1) + (A_2+A_3).(1-D \\ -\hat{d}).(x+\hat{x})] + [(B_1.(2(D+\hat{d})-1) + (B_2+B_3) \\ .(1-D-\hat{d}).(u+\hat{u})] \end{aligned} \quad (34)$$

By ignoring small perturbations in small-signal model (34), it transformed in (35),

$$\begin{aligned} \hat{\dot{x}} = (2.\hat{d}.A_1 - \hat{d}.(A_2+A_3)).x + (A_1.(2D-1) \\ +(A_2+A_3).(1-D)).\hat{x} + (2.\hat{d}.B_1 - \hat{d}.(B_2+B_3)). \\ u + (B_1.(2D-1) + (B_2+B_3). \\ (1-D)).\hat{u} \end{aligned} \quad (35)$$

Laplace Transformation of (35) is given in (36),

$$\begin{aligned} s.\hat{x(s)} = A.\hat{x(s)} + B.\hat{u(s)} + [(2.A_1 - A_2 - A_3).x \\ +(2.B_1 - B_2 - B_3).u].\hat{d(s)} \end{aligned} \quad (36)$$

ISBN: 978-988-14048-8-6
ISSN: 2078-0958 (Print); ISSN: 2078-0966 (Online)

Equation (37) can be obtained by rearranging (36)

$$\hat{x(s)} = (sI - A)^{-1}.[B.\hat{u(s)} + (2.A_1 - A_2 - A_3).x + (2.B_1 - B_2 - B_3).u].\hat{d(s)} \quad (37)$$

Let

$$L = 2.A_1 - A_2 - A_3 \quad (38)$$

$$M = 2.B_1 - B_2 - B_3 \quad (39)$$

Put (38) and (39), in (37), to get (40),

$$\hat{x(s)} = (sI - A)^{-1}.[B.\hat{u(s)} + L.x + M.u].\hat{d(s)} \quad (40)$$

output equation given in (9) can b written as (41)

$$\hat{y} = (C_1.(2(D+\hat{d})-1)+(C_2+C_3).(1-D-\hat{d}).(x+\hat{x}) \quad (41)$$

where,

$$\hat{y} = Y + y \quad (42)$$

and

$$Y = [C_1.(2D + -1) + (C_2 + C_3).(1 - D)].x \quad (43)$$

By ignoring small perturbation of (42) and (43), (44) can be achieved.

$$\hat{y} = [C_1.(2D + -1) + (C_2 + C_3).(1 - D)].\hat{x} + [(2.C_1 - (C_2 + C_3)).x].\hat{d} \quad (44)$$

Let

$$N = [C_1.(2D + -1) + (C_2 + C_3).(1 - D)] \quad (45)$$

and

$$O = 2.C_1 - C_2 - C_3 \quad (46)$$

put (45) and (46) in (44) get (47)

$$\hat{y} = [N].\hat{x} + [O.x].\hat{d} \quad (47)$$

Equation (48) can be achieved from (40)

$$\hat{x(s)} = N.(sI-A)^{-1}.[B.\hat{u(s)}+L.x+M.u].\hat{d(s)}+[O.x].\hat{d(s)} \quad (48)$$

If

$$B.\hat{u(s)} = 0 \quad (49)$$

Then, by substituting (49) in (48) will get (50) which defined the transfer function

$$\frac{\hat{y}}{\hat{d(s)}} = N.(sI - A)^{-1}.[(L).x + (M).u + (O).x] \quad (50)$$

This transfer-function can be obtained using design requirements of IBBC given in Table II.

III. Controller Design

Interleaved Buck-Boost Converter is a Non-minimal phase and open-loop unstable system. Due to these inherent properties controller designing of this system is a challenging task. In Non-minimal phase, zeroes of the system are at right-hand side of the s-plane. This system can be demonstrated in two different ways as shown in Fig. 4 and Fig. 5

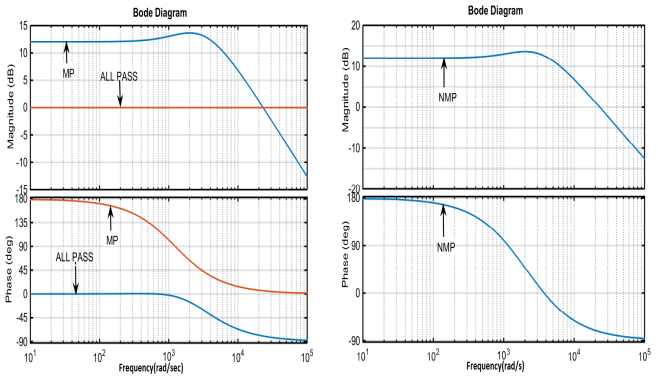

(a) Bode-plot of All-pass and Minimal phase system (b) Bode-plot of Non-minimal phase system

Fig. 4: Fequency-response of III-A representation

A. I^{st} method

$$G_{NMP1} = K\frac{\frac{s}{\omega_1} - 1}{(\frac{s}{\omega_2} + 1).(\frac{s}{\omega_3} + 1)} \quad (51)$$

A Non-minimal phase system (51) can be written as a product of minimal system and all-pass system as shown in (52) and (53).

$$G_{MP1} = K\frac{\frac{s}{\omega_1} + 1}{(\frac{s}{\omega_2} + 1).(\frac{s}{\omega_3} + 1)}; G_{AP1} = \frac{-\frac{s}{\omega_1} + 1}{(\frac{s}{\omega_1} + 1)}; \quad (52)$$

Here-

$$G_{NMP1} = G_{MP1} * G_{AP1} \quad (53)$$

B. II^{nd} method

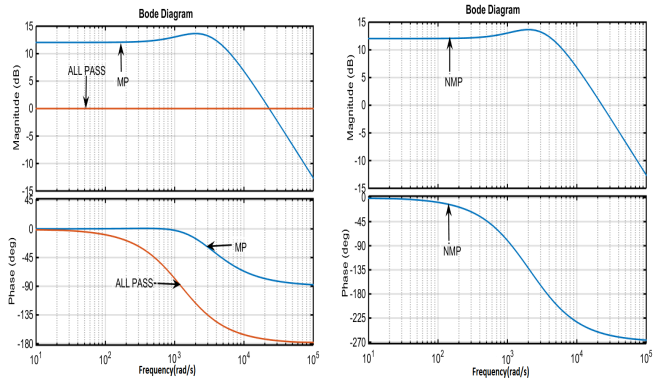

(a) Bode-plot of All-pass and Minimal phase system (b) Bode-plot of Non-minimal phase system

Fig. 5: Fequency-response of III-B representation

$$G_{NMP2} = K\frac{-\frac{s}{\omega_1} + 1}{(\frac{s}{\omega_2} + 1).(\frac{s}{\omega_3} + 1)} \quad (54)$$

A Non-minimal phase system (54) can be written as a product of minimal system and all-pass system as shown in (55) and (56).

$$G_{MP2} = K\frac{\frac{s}{\omega_1} + 1}{(\frac{s}{\omega_2} + 1).(\frac{s}{\omega_3} + 1)}; G_{AP2} = \frac{-\frac{s}{\omega_1} + 1}{(\frac{s}{\omega_1} + 1)}; \quad (55)$$

ISBN: 978-988-14048-8-6
ISSN: 2078-0958 (Print); ISSN: 2078-0966 (Online)

Here-

$$G_{NMP2} = G_{MP2} * G_{AP2} \tag{56}$$

Both representations shown in $Fig-4$ and $Fig-5$, represent same system but as it is desired to cut phase-plot at -180^0, so it is obvious that second representation is the correct representation. By using second representation of NMP-system a controller has to be designed using Loop-shaping method. In Loop-Shaping, explicitly shape the magnitude of the loop transfer function $|L(j\omega)|$ has to be drawn.

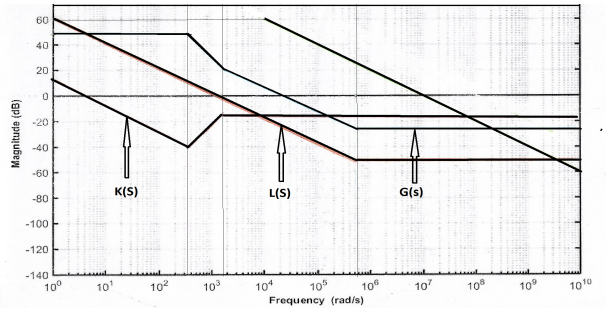

Fig. 6: Magnitude plot of system without controller($G(s)$), controller($K(s)$) and system with contoller($L(s)$) mentioned in (57) and (58) respectively

Here $L(s) = G(s).K(s)$, where $G(s)$-transfer-function of the plant and $K(s)$-Feedback controller to be designed mentioned in (57) and (58). In bandwidth region $|L(j\omega)|$ has to be as large as possible to get the benefits of feedback controller. To design a controller with loop-shaping, a slope of -20db/decade has been extended for 6 decades to get operating frequency before cut-off frequency. Rest of the plot will remain same. The frequency response (Bode-plot) of the plant and loop-shape is shown in Fig. 6.

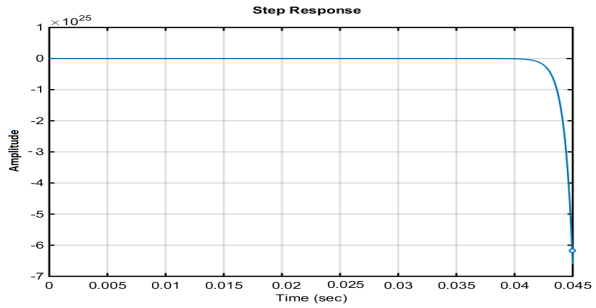

Fig. 7: Time response of system without controller

$$G(s) = \frac{0.04154.(s+35400).(s-1484)}{s^2+163.6.s+151800}$$
$$K(s) = -\frac{4.624.(6.58*10^{-6}.s^2+1.077*10^{-3}.s+1)}{s.(6.73*10^{-4}.s+1484)} \tag{57}$$

Controller gain was selected to have appropriate stability margins(PM and GM)

$$L(s) = \frac{0.00185.(s+35400)(s-1484)}{s.(s+1484)} \tag{58}$$

The controller has zeroes at same position where plant poles are situated as drop in the slope of loop-shape at break frequencies, just before crossover is not desired.

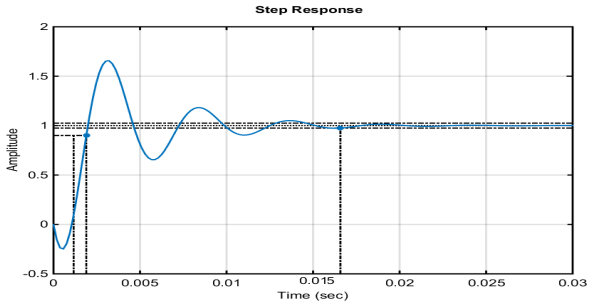

Fig. 8: Time response of system with feedback-controller

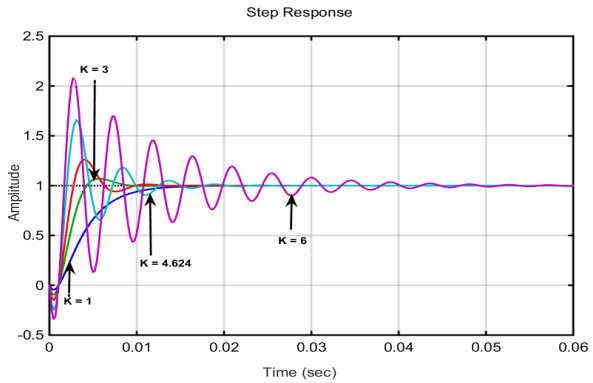

Fig. 9: Time response of system with feedback-controller with variation in Gain of controller (K_c)

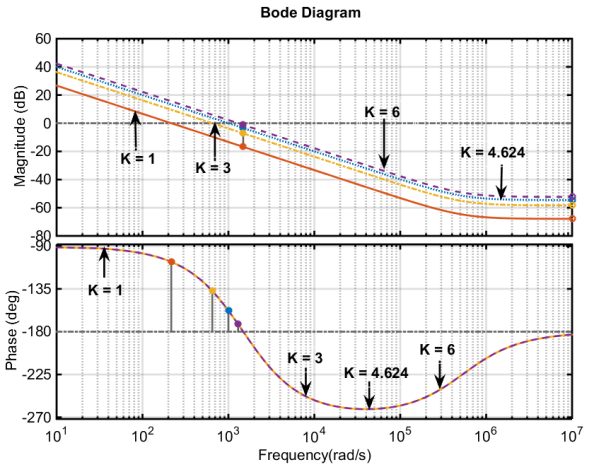

Fig. 10: Variation in phase-margin

IV. Results and Discussions

InterleavedBuck-boost Converter is a non-minimal and unstable open-loop system with PM 96.6^0 and GM $-46.8dB$. By using Loop-shaping method, the author has been designed a controller which makes closed loop system stable with PM 22.1^0 and GM 3.44dB as shown in Fig.10.This controller not only make close loop stable system but also improves time-response of the system.

Initially the open loop system has shown an unstable behavior as shown in Fig. 7. It is shown in the Fig. 8 that after using controller system becomes stable with settling time (T_s=0.0166sec) and Maximum-overshoot (M_p=65.61). Fig.9 and 10 shows the variation in time response and frequency response respectively with variation in gain K.

ISBN: 978-988-14048-8-6
ISSN: 2078-0958 (Print); ISSN: 2078-0966 (Online)

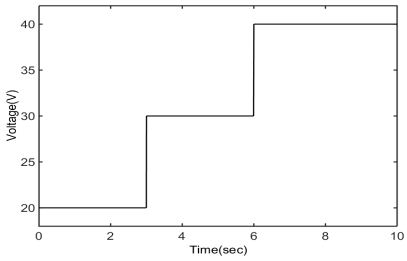

(a) Input Voltage V_{in}

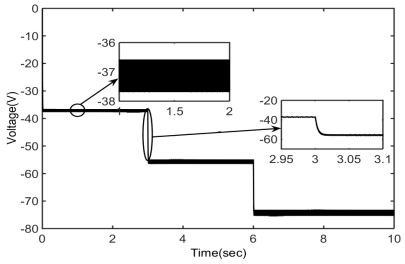

(b) Output Voltage V_{out}

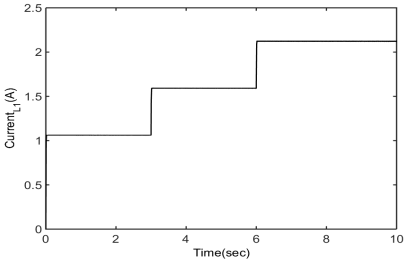

(c) Inductor current I_{L1} and I_{L2}

Fig. 11: Wave-forms without controller

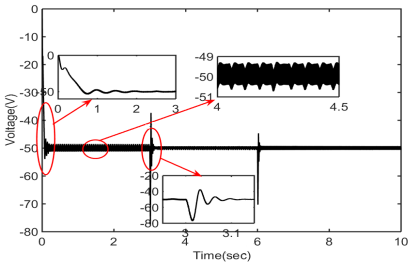

(a) Output Voltage V_{out}

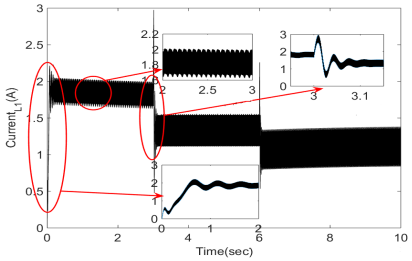

(b) Inductor current I_{L1}

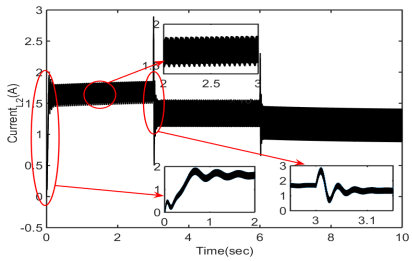

(c) Inductor current I_{L2}

Fig. 12: Wave-forms with controller

A. *Simulation Results*

Fig. 11 is presenting the simulation results of voltage (V_o), inductor currents (I_{L1}, I_{L2}) with respect to the variation in input voltage (V_s) without controller. It is observed that with change in input voltage as shown in Fig. 11a, the output voltage shown in 11b is also changing, which is not a desired consequence. Therefore, a controller using loop-shaping is designed to achieve the desired behaviour. Fig. 11c shows the inductor currents.

As shown in fig12, when controller is applied to the system, output voltage(V_{out}) stabilizes at V=-50V irrespective of the change in input voltage. Due to switching action some transient behavior is also present in the waveform which is shown in Fig. 12a. Desired ripple in the Voltage-waveform is set to be 10% of the output voltage which can be seen in the Fig. 12a. Ripple in inductor currents is also set to be 10% of output current which is shown in the fig12b and fig12c.

V. Conclusion

In this study, a compensator has been designed for NMP Interleaved Buck-boost Converter (IBBC) using a graphical loop-shaping technique. It is found that without any mathematical calculation a suitable compensator has been designed which makes the close-loop stable system with GM 3.44dB, and PM 22.1^0. This controller also improves time-response curve with settling-time 0.0166sec and maximum-overshoot 65.61.

References

[1] Dynamic modelling of a quadratic DC/DC single-switch boost Converter.
[2] Simulation of Buck-Boost Converter for Solar Panels using PID Controller 3rd ed. Harlow, England: Addison-Wesley, 1999.
[3] A novel low-ripple Interleaved Buck–Boost Converter with high efficiency and low oscillation for fuel-cell applications Vahid Samavatian,Ahmad Radan
[4] Hybrid-mode Interleavedboost Converter design for fuel cell electric vehicles.
[5] Analysis, modeling and implementation of an Interleaved Boost DC-DC Converter for fuel cell used in electric vehicle
[6] Minimize Current Stress of Dual-Active-Bridge DC-DC Converters for Electric Vehicles Based on Lagrange Multipliers Method
[7] Research on Control Strategy of the Bidirectional Full-bridge DC/DC Converter Used in Electric Vehicles
[8] An overview of high voltage conversion ratio DC-DC Converter configurations used in DC micro-grid architectures.
[9] DC/DC Converter topologies for electrolyzers: State-of-the-art and remaining key issues
[10] A Novel Efficiency Modeling Method for a DC-DC Converter in the Hybrid Energy Storage System for Electric Vehicles
[11] Real-time implementation of four-phase InterleavedDC–DC boost Converter for electric vehicle power system
[12] FPGA based fault-tolerant control on an InterleavedDC/DC boost Converter for fuel cell electric vehicle applications
[13] A new controller for DC-DC Converters based on particle swarm optimization.
[14] Improved dynamic response of isolated full bridge DC to DC Converter using BATA optimization tuned fuzzy sliding mode controller for solar applications
[15] GA-based robust LQR controller for Interleavedboost DC–DC Converter improving fuel cell voltage regulation.
[16] FPGA-based optimal robust minimal-order controller structure.

ISBN: 978-988-14048-8-6
ISSN: 2078-0958 (Print); ISSN: 2078-0966 (Online)